AIAA Journal
Vol. 56, No. 7, July 2018

Technical Notes

Oscillation Modes in Screeching Jets

Romain Gojon*
KTH Royal Institute of Technology, SE-100 44 Stockholm, Sweden
Christophe Bogey†
École Centrale de Lyon, 69134 Ecully Cedex, France
and
Mihai Mihaescu‡
KTH Royal Institute of Technology, SE-100 44 Stockholm, Sweden

DOI: 10.2514/1.J056936

I. Introduction

Nonideally expanded supersonic jets generate three basic noise components, namely, the turbulent mixing noise, the broadband shock-associated noise, and the screech noise [1]. The mixing noise, obtained for both subsonic and supersonic jets, is most intense in the downstream direction; and it occurs at Strouhal numbers of around 0.15. The broadband shock-associated noise is radiated mainly in the radial direction, and it has a central frequency varying with the emission angle. The screech noise consists of tones measured in the upstream direction. These tones are due to an aeroacoustic feedback mechanism establishing between turbulent structures propagating downstream and acoustic waves propagating upstream, which was described by Powell [2] and then by Raman [3], among others. According to these authors, the structures developing in the jet shear layers interact with the quasi-periodic shock-cell structure of the jet, which creates upstream-propagating acoustic waves. The sound waves are reflected back at the nozzle lips, which excites the shear layers and closes the feedback loop.

At the screech tone frequencies, the jets undergo strong oscillations. For round jets, Powell [2] identified four oscillation modes (A, B, C, and D) on the basis of the variations of the screech frequency with the jet ideally expanded Mach number $\mathcal{M}_j$. Each mode was observed over a specific range of Mach number, and frequency jumps were noted between the modes. Later, Merle [4] showed that mode A could be divided into modes $A1$ and $A2$. Davies and Oldfield [5] studied the oscillation modes of the jets associated with the screech modes. They found that modes $A1$ and $A2$ corresponded to axisymmetric oscillation modes, mode C corresponded to helical modes, and modes B and D corresponded to flapping and sinuous modes. Powell et al. [6] and Tam et al. [7] suggested that the mode switching phenomenon was due to the change in the growth rate of the shear-layer instability waves as $\mathcal{M}_j$ varied. Using numerical simulations, Shen and Tam [8] also provided evidence that two screech tones could coexist. As an explanation, they proposed that there were two ways by which the screech feedback loop was accomplished. In the first one, the feedback acoustic waves were generated by the interactions between the jet instability waves and the shock-cell structures, as was done for the broadband shock-associated noise. Using the formula [9] giving the frequency of this noise in the upstream direction, good agreement was thus noticed for the frequencies of screech modes $A1$ and B. In the second way to complete the screech loop, the feedback link was provided by upstream-propagating acoustic wave modes of the jets. By comparing the screech tone wavelengths predicted when the frequency of these modes was calculated using a vortex sheet model of the ideally expanded equivalent jet with experimental data, Shen and Tam [8] showed that this was most probably the case for screech modes $A2$ and C. However, the acoustic modes of the ideally expanded equivalent were not directly observed in the jet.

In this Note, the origin of the oscillation modes of screeching round jets is investigated by assuming that the feedback part of the aeroacoustic loop responsible for screech noise can be modeled by considering the neutral acoustic wave modes of the equivalent ideally expanded jets, as in the work of Shen and Tam [8]. Such modes are characterized in Sec. II by a simple wave analysis using a vortex sheet model. The validity of the present assumption is assessed from reference experimental data in Sec. III, as well as from simulation results in Sec. IV. In the latter section, an attempt is made to detect upstream-propagating waves in a screeching jet, as was done recently in ideally expanded impinging jets [10]. In particular, based on the frequency-wave-number spectra of density fluctuations, high-amplitude patterns corresponding to neutral acoustic wave modes of the ideally expanded equivalent jet are observed inside the jet, for the first time (to the best of our knowledge), in nonideally expanded jets. Concluding remarks are given in Sec. V.

II. Modeling of the Feedback Waves in Screeching Jets

In the present Note, as in the work by Shen and Tam [8], it is assumed that the feedback loop causing screech noise in nonideally expanded jets is closed by acoustic waves belonging to the family of the upstream-propagating acoustic wave modes of the equivalent ideally expanded jet. This hypothesis seems natural, given that, experimentally [2,4,5,11,12], the screech frequencies and the corresponding oscillation modes of the jets depend primarily on the ideally expanded Mach number of the jets.

The dispersion relations of these instability waves are approximated by using a vortex sheet model of the jets as proposed by Lessen et al. [13]. By starting from the linearized governing equations for a compressible inviscid fluid, and noting that the waves are neutral for a vortex sheet model (i.e., that they have both a real wave number k and angular frequency ω), these authors obtained the following relations for an ideally expanded round jet of diameter D_j, exit velocity u_j, and Mach number $\mathcal{M}_j$:

$$|\xi_+|J_n(|\xi_-\alpha|)\frac{K_{n-1}(|\xi_+\alpha|)+K_{n+1}(|\xi_+\alpha|)}{K_n(|\xi_+\alpha|)} + \frac{C^2|\xi_-|}{(a_0C/a_j-\mathcal{M}_j)^2}[J_{n-1}(|\xi_-\alpha|)-J_{n+1}(|\xi_-\alpha|)] = 0 \quad (1)$$

where a_0 and a_j are the sound speeds in the ambient medium and in the jet, $C=\omega/(ka_0)$, J_n is the nth order Bessel function of the first kind,

Received 13 November 2017; revision received 8 February 2018; accepted for publication 8 March 2018; published online 27 April 2018.

*Research Associate, Department of Mechanics, Linné FLOW Centre; also Département Aérodynamique, Energétique et Propulsion-DAEP ISAE-SUPAERO, Université de Toulouse, 10 Avenue Edouard Belin, 31400 Toulouse, France; romain.gojon@isae-supaero.fr. Member AIAA.

†Research Scientist, Laboratoire de Mécanique des Fluides et d'Acoustique, UMR CNRS 5509; christophe.bogey@ec-lyon.fr. Senior Member AIAA.

‡Associate Professor, Department of Mechanics, Linné FLOW Centre; mihai@mech.kth.se. Senior Member AIAA.

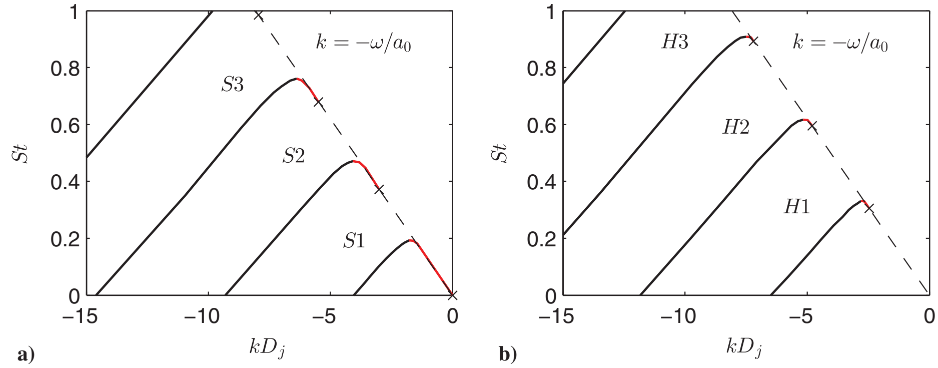

Fig. 1 Dispersion relations of a) axisymmetric and b) helical neutral acoustic wave modes; (×) lower limits of the modes, (dashed) $k = -\omega/a_0$.

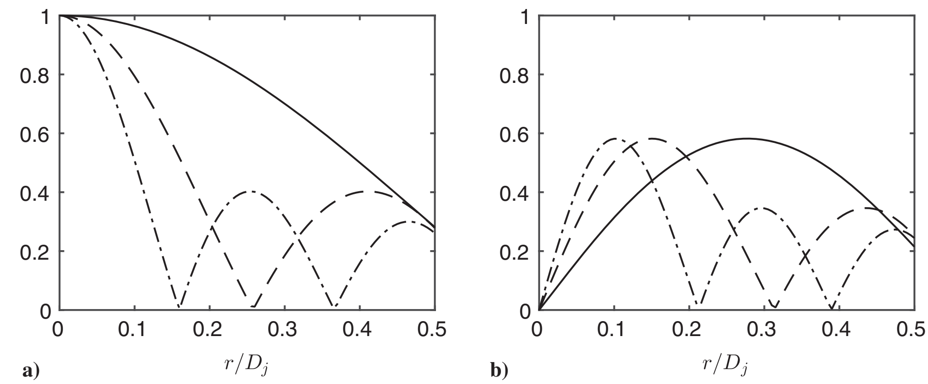

Fig. 2 Eigenfunction distributions of neutral acoustic modes: a) axisymmetric modes $S1$ (solid line), $S2$ (dashed), and $S3$ (dash–dotted); and b) helical modes $H1$ (solid line), $H2$ (dashed), and $H3$ (dash–dotted).

$\xi_+ = |C^2 - 1|^{1/2}$, $\xi_- = |(a_0 C/a_j - \mathcal{M}_j)^2 - 1|^{1/2}$, $\alpha = kD_j/2$, and K_n is the nth order modified Bessel function.

The dispersion relations obtained for a round jet at a Mach number of $\mathcal{M}_j = 1.56$ (similar to the screeching jet to be considered in Sec. IV) for the axisymmetric modes ($n = 0$) and the first helical modes ($n = 1$) are represented in Fig. 1 as functions of the Strouhal number $St = fD_j/u_j$ and the wave number kD_j, where f is the frequency. As pointed out by Tam and Hu [14], discrete acoustic modes can be seen. More precisely, an infinite number of modes exist, and they can be ordered by increasing Strouhal numbers of their lower limits. The lower limits of the modes, given by Tam and Ahuja [15], are also represented in Fig. 1. Within the frequency range considered, three axisymmetric neutral acoustic wave modes (referred to as $S1$, $S2$, and $S3$) and three helical modes (denoted by $H1$, $H2$, and $H3$) appear.

For the different modes, the upstream-propagating acoustic waves are situated on the part of the dispersion curves colored in red, where the slope $\mathrm{d}St/\mathrm{d}k$ and, hence, the group velocity $\mathrm{d}\omega/\mathrm{d}k$ are negative, which leads to the existence of allowable frequency ranges.

Typical eigenfunction distributions obtained for axisymmetric modes $S1$, $S2$, and $S3$ and helical modes $H1$, $H2$, and $H3$ are plotted in Fig. 2 as a function of the radial distance. They are calculated here for the maximum Strouhal number of each mode, but the results are similar for other positions on the same mode.

III. Assessment of the Modeling Using Experimental Data

The allowable frequency ranges obtained for the axisymmetric and the helical upstream-propagating neutral wave modes are represented in Fig. 3 as a function of the Mach number $\mathcal{M}_j$. They are determined from the maximum and minimum Strouhal numbers of each mode, which are taken from the dispersion curves in the first case, and are calculated in the second case as in the work of Tam and Ahuja [15]. To assess the validity of the modeling proposed by Shen and Tam [8] and examined in the present Note, the tone frequencies acquired in the reference experiments of Powell et al. [6] and Ponton and Seiner [16] for different screech modes are also depicted. For Ponton and Seiner [16], the results represented were those for jets with a nozzle thickness equal to $0.625D$, where D was the exit diameter. The semiempirical relation developed by Tam et al. [9] was also plotted in the figure. The relations are written as

$$St = \frac{0.62}{(\mathcal{M}_j^2 - 1)^{1/2}}\left[1 + 0.65\mathcal{M}_j\left(1 + \frac{\gamma - 1}{2}\mathcal{M}_j^2\right)^{-1/2}\left(\frac{T_0}{T_r}\right)^{-1/2}\right]^{-1} \tag{2}$$

where T_0 and T_r are the ambient temperature and the total temperature of the jet, respectively; $\gamma = 1.4$ is the ratio of specific heats; and a mean convection velocity equal to 65% of the ideally expanded jet velocity is considered.

Overall, as observed by numerous researchers [11,12,17], the screech frequency decreases with the ideally expanded Mach number [9], following the semiempirical relation developed by Tam et al. [9]. Moreover, the variations of the screech frequencies with $\mathcal{M}_j$ closely follow those of the allowable frequency ranges. This is the case for the dominant screech mode C in both experiments and for the secondary screech mode c in the experiment of Powell et al. [6], for which the frequencies strikingly fall on the line corresponding to the lower limit of the band for the helical mode $H1$. This is also true for dominant screech modes $A1$ and $A2$ and secondary screech mode u, for which the frequencies are located near the lower limit of the band for axisymmetric mode $S2$. These results suggest that the former screech modes are helical and that the latter are axisymmetric, which is in agreement with experimental observations for screech modes $A1$, $A2$, C, and c, as well as with expectations [6] for screech mode u. It is interesting to note that the screech tones are located mainly near the lower limits of the allowable frequency ranges. At these positions, the neutral upstream-propagating acoustic waves have group and phase velocities both close to the ambient speed of sound. In the present

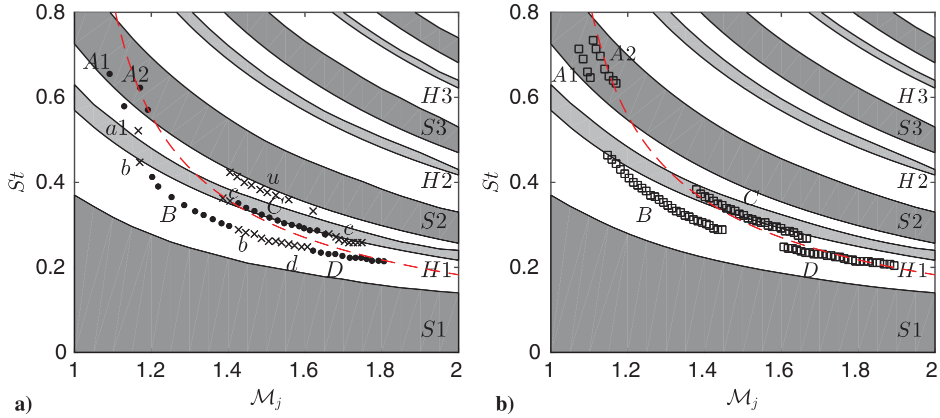

Fig. 3 Allowable frequency ranges for the axisymmetric (dark gray) and helical (light gray) upstream-propagating neutral acoustic modes; tone frequencies (symbols) in experiments a) [6] and b) [16]; (red dashed) semi empirical relation [9].

model, the waves closing the feedback loop therefore appear to propagate at the same speed as the acoustic waves considered to complete the loop outside the jet flow in the classical screech mechanism model [2,3].

Similar observations have been made by Tam and Norum [18], Gojon et al. [19], and Bogey and Gojon [10] for impingement tones in supersonic ideally expanded jets. It thus appears that the present modeling of the feedback waves allows us to predict the variations of the frequencies of these screech modes with $\mathcal{M}_j$, as well as their axisymmetric or helical natures. Note that the frequencies of screech modes B and D, as well as of modes b and d, lie outside the allowable frequency ranges for the axisymmetric and helical upstream-propagating neutral acoustic wave modes. This can be explained by the fact that these modes are associated with more complex flapping/sinuous jet oscillation modes.

IV. Further Assessment of the Modeling Using Numerical Data

The results obtained for a round screeching jet in a recent study [20] using large-eddy simulation (LES) are now examined.

A. Parameters and Methods

At the exit of a straight pipe nozzle with a diameter of $D = 2r_0 = 2$ mm and a thickness of $0.1r_0$, the jet is characterized by a nozzle pressure ratio of $p_r/p_0 = 4.03$ and a temperature ratio of $T_r/T_0 = 1$, where suffixes r and 0 denote, respectively, stagnation and ambient values. The jet is underexpanded; has a fully expanded Mach number of $\mathcal{M}_j = u_j/a_j = 1.56$; an exit Mach number of $\mathcal{M}_e = 1$ (i.e., it simulates a jet exiting from a convergent nozzle); and a Reynolds number of $Re_j = u_j D_j/\nu_j = 6 \times 10^4$, where u_j and a_j are the velocity and the speed of sound in the equivalent ideally expanded jet with a diameter of $D_j = 2.2$ mm; and ν_j is the kinematic molecular viscosity.

The LES is performed by solving the unsteady compressible Navier–Stokes equations on a cylindrical mesh (r, θ, z). The time integration and spatial derivation are performed using an explicit six-stage Runge–Kutta algorithm and low-dispersion and low-dissipation explicit finite differences [21,22], respectively. At the end of each time step, a high-order filtering is applied to the flow variables in order to remove grid-to-grid oscillations and to dissipate subgrid-scale turbulent energy [23–25]. The boundaries are treated with the radiation conditions of Tam and Dong [26], and a sponge zone is employed to damp the turbulent fluctuations. No-slip adiabatic conditions are imposed at the nozzle walls. Finally, a shock-capturing filtering is applied in order to avoid Gibbs oscillations near shocks [27]. The simulation has been carried out using an OpenMP-based in-house code solving the unsteady compressible Navier–Stokes equations in cylindrical coordinates (r, θ, z) using low-dispersion and low-dissipation finite difference schemes [21,27–29]. The mesh contains 400 million points, and it exhibits a minimal spacing of $0.0075r_0$ in the jet shear layers and at the nozzle exit, as well as a maximum spacing of $0.06r_0$, allowing properly propagated acoustic waves with Strouhal numbers up to $St = fD_j/u_j = 5.3$. The simulation time, after the transient regime, is equal to $500D_j/u_j$.

B. Flow Snapshot and Near-Nozzle Pressure Spectrum

Three isosurfaces of density in the jet flow and the pressure fluctuations in the planes $\theta = 0$ and $\theta = \pi$ are represented in Fig. 4. In the jet, a shock-cell structure and the jet mixing layers are well visible. Outside, strong acoustic waves clearly appear to propagate in the upstream direction. More information about the hydrodynamic and acoustic fields of the jet can be found in a dedicated paper [20].

The pressure spectrum obtained near the nozzle exit at $z = 0$ and $r = 2r_0$ is displayed in Fig. 5 as a function of the Strouhal number. Two tones emerge 15 dB above the broadband noise at Strouhal numbers of $St_1 = 0.28$ and $St_2 = 0.305$, and a secondary tone is found at $St_3 = 0.38$. Such a result is typical of a screeching jet; see, for instance, in the work of Westley and Woolley [11], Panda [12], and André [17]. Moreover, Eq. (2) gives $St = 0.285$ for the simulated jet, which is in good agreement with the frequency of the two dominant tones. The present jet thus generates screech tones. According to the classification of the screech modes used in Fig. 3, the two dominant tones belong to mode C, and the secondary tone belongs to mode u. An in-depth analysis of those tones was given in a previous paper [20].

C. Near-Pressure Field

A Fourier transform has been applied to the near-pressure field recorded in the (z, r) plane in order to determine the amplitude and

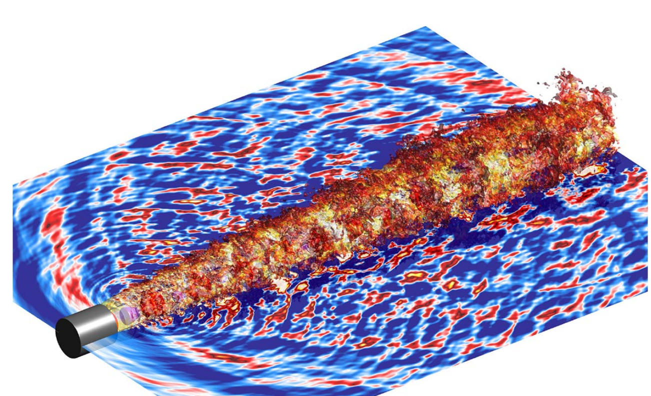

Fig. 4 Density isosurfaces for 0.8 and 2.5 $\mathrm{kg \cdot m^{-3}}$ (purple and red) and 1.25 $\mathrm{kg \cdot m^{-3}}$ colored by the Mach number; pressure fluctuations at $\theta = 0$ and π using a color scale from −2000 to 2000 Pa from blue to red; nozzle in gray.

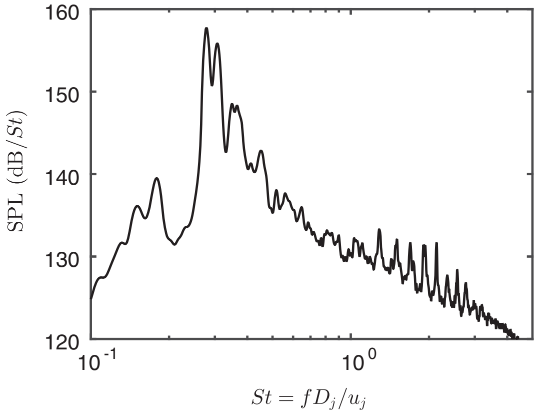

Fig. 5 Sound pressure levels (SPLs) obtained at $z = 0$ and $r = 2r_0$ as a function of Strouhal number St.

phase fields associated with the different screech tones. These fields are represented in Fig. 6.

At the three tone frequencies, the amplitude fields in Figs. 6a–6c exhibit cell structures. Such structures have been observed, for instance, experimentally by Panda et al. [30] in screeching jets and numerically by Gojon et al. [19] in ideally expanded planar impinging jets. They are due to the formation of hydrodynamic–acoustic standing waves. The levels on the jet axis are negligible at the two first frequencies but strong at the third one. The phase fields of Figs. 6d–6f, as well as the results obtained using Fourier decomposition in the azimuthal direction at $z = 0$ and $r = 2r_0$ (not shown here for brevity), provide additional information on the spatial organization of the pressure field. They indicate that the jet undergoes helical oscillations at $St_1 = 0.28$ and $St_2 = 0.305$ but an axisymmetric oscillation at $St_3 = 0.38$. These findings are consistent with the screech modes associated with the different tones, namely, mode C for the two first tones and mode u for the third tone. In particular, the axisymmetric nature of the mode u suggested by the model in Sec. II clearly appears.

D. Wave-Number-Frequency Density Spectra in the Jet

To detect upstream-propagating waves in the present jet, as was recently done by Towne et al. [31] in a subsonic free jet and by Bogey and Gojon [10] in ideally expanded impinging jets, a space–time Fourier transform has been applied to the density fluctuations at different radial positions between $r = 0$ and $r = r_0$ along a line extending from the axial position of $z = 0$ to $z = 10r_0$. The frequency-wave-number spectra obtained for azimuthal modes of $n = 0$ and $n = 1$ at $r = 0.1r_0$, $r = 0.5r_0$, and $r = r_0$ are represented in Fig. 7 as functions of the Strouhal number of $St = fD_j/u_j$ and of the normalized axial wave number kD_j. Only the negative wave number part is shown. The dispersion relations of the neutral acoustic wave modes of the equivalent ideally expanded jet are also displayed. For the azimuthal mode of $n = 0$, significant levels are found in Figs. 7a, 7c, and 7e that are slightly above the theoretical curves associated with modes $S1$ and $S2$. The discrepancies with respect to the model may be due to the presence of shock motions in the simulated jets, as well as to the use of an infinitely thin shear layer in the vortex sheet model [15,10]. Moreover, the amplitude of those bands decreases with the radial position at which the frequency-wave-number spectrum is represented, following the eigenfunction distributions in Fig. 2a. In Figs. 7b, 7d, and 7f for the azimuthal mode of $n = 1$, strong components appear along mode $H2$ at $r = 0.1r_0$ in Fig. 7b and along modes $H1$ and $H2$ at $r = 0.5r_0$ in Fig. 7d. Those results are again in agreement with the eigenfunction distributions of the two first helical neutral acoustic wave modes in Fig. 2b.

The eigenfunction profiles presented in Fig. 2 are now compared with the adimensional amplitude profiles extracted from the frequency-wave-number spectra of density fluctuations at 11 radial positions from $r = 0$ to $r = r_0$. They are estimated at the tone Strouhal numbers of $St = 0.38$ and $St = 0.28$ for $S2$ and $H1$, respectively, and at the maximum Strouhal number of the mode for $S1$ and $H2$. In the first case, the amplitude seems to be well converged because of the high-energy content at the tone Strouhal numbers. In the latter case, the maximum Strouhal number corresponds to the position where the eigenfunction profiles have been calculated using the vortex sheet model. The comparisons are given in Fig. 8. A good agreement is obtained for all the modes. The same observation has been made for round, ideally expanded, impinging jets [10] where the amplitude fields obtained for the pressure fluctuations at the tone frequencies bear similarities with the eigenfunction distributions of the neutral acoustic wave modes of the jet. These results provide strong evidence, for the first time (to the best of the authors' knowledge), that a vortex sheet model of the corresponding ideally expanded jet is capable of predicting the wave modes of a nonideally expanded supersonic jet. However, among those waves, the ones with a positive group velocity that have been observed in Fig. 7 cannot be involved in the proposed feedback loop model.

Peak levels are reached in the spectra on the line $k = -\omega/a_0$ at the Strouhal number of $St_3 = 0.38$ of the axisymmetric screech tone for the azimuthal mode of $n = 0$ in Figs. 7a, 7c, and 7e, as well as at the Strouhal numbers of $St_1 = 0.28$ and $St_2 = 0.305$ of the helical screech tones for the mode of $n = 1$ in Figs. 7a, 7c, and 7e. They are located very near the lower limits of the dispersion relations of the neutral acoustic wave modes of the equivalent ideally expanded jet. Therefore, the associated waves propagate upstream inside the jet with group and phase velocities both close to the ambient speed of sound.

In the spectra of Fig. 7, energy is distributed along a wide range of spatial wave numbers for each tonal frequency, which seems in contradiction with the model proposed by Shen and Tam [8] and in the present Note, in which the waves closing the feedback loop exist only at a single wave number for each frequency. This is most likely due to the interaction of the upstream-propagating acoustic waves with the turbulence in the jet shear layer and the shock cells, which leads to a redistribution of the energy to the close wave numbers. To quantify the energy redistribution in the wave number space, the spectra of the density fluctuations are plotted in Fig. 9 as a function of

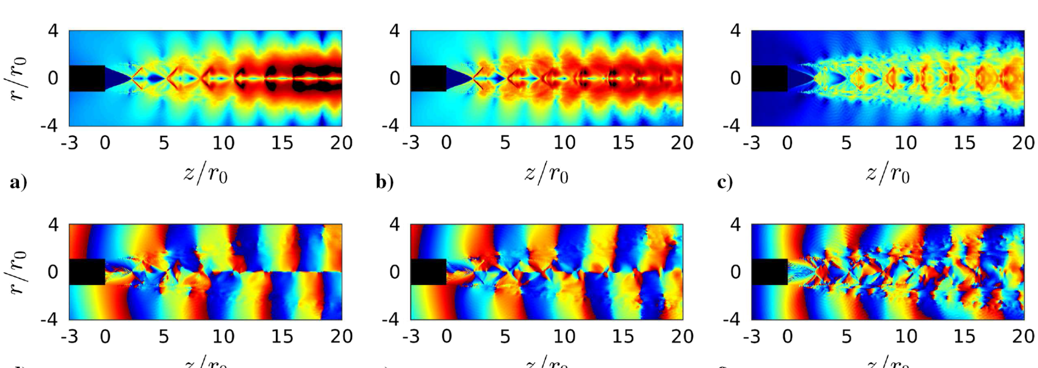

Fig. 6 a–c) Amplitude and d–f) phase fields obtained for the pressure fluctuations at a,d) $St_1 = 0.28$, b,e) $St_2 = 0.305$, and c,f) $St_3 = 0.38$, using color scales from 60 to 100 dB/St and $-\pi$ to π from blue to red.

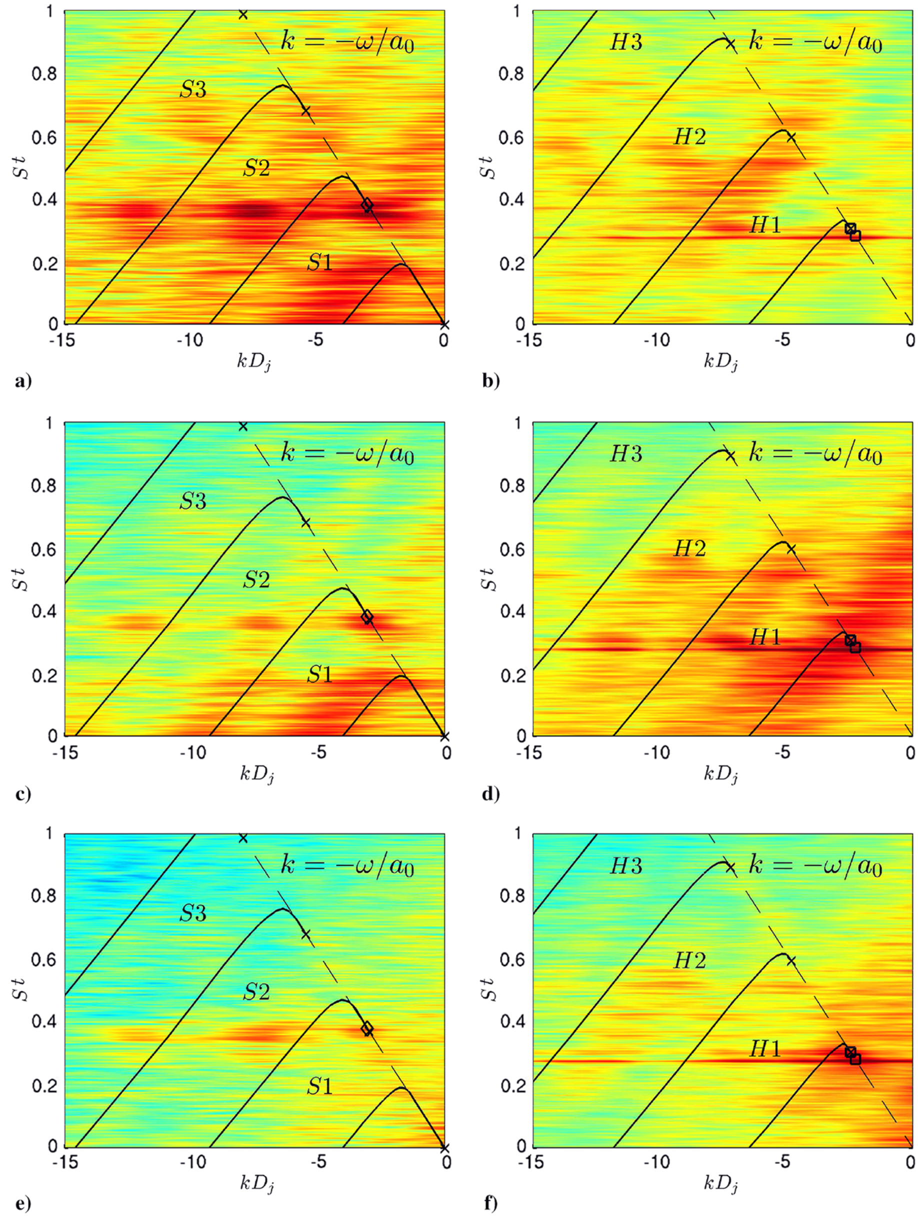

Fig. 7 Frequency-wave-number spectra of density fluctuations at a,b) $r = 0.1r_0$, c,d) $r = 0.5r_0$, and e,f) $r = r_0$ for modes a,c,e) $n = 0$ and b,d,f) $n = 1$; (solid lines) dispersion relations of the axisymmetric (left) and helical (right) neutral acoustic modes; (×) mode lower limits; (dashed) $k = -\omega/a_0$; screech tone frequencies for axisymmetric (diamonds) and helical (squares) modes; color-scale levels over 60 dB from blue to red.

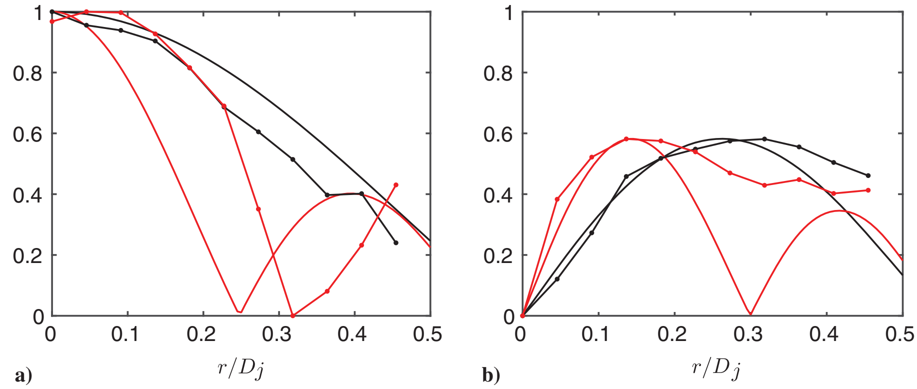

Fig. 8 Eigenfunction distributions of the neutral acoustic modes: a) axisymmetric modes $S1$ (black line) and $S2$ (red line), and b) helical modes $H1$ (black line) and $H2$ (red line); (solid dotted line) results from the LES.

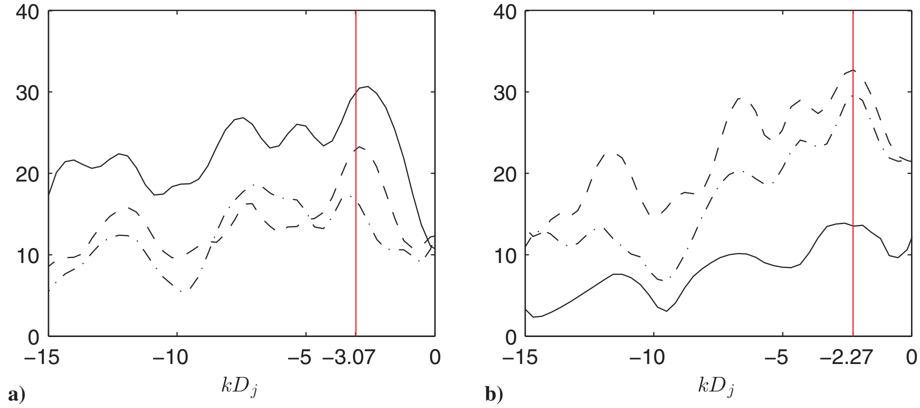

Fig. 9 Wave number spectra of density fluctuations for modes a) $n = 0$ at $St = 0.38$ and b) $n = 1$ at $St = 0.28$: at (black solid lines) $r = 0.1r_0$, (dashed) $r = 0.5r_0$, and (dashed–dotted) $r = r_0$; (red solid line) wave number linked to the frequency localized on the corresponding neutral acoustic mode (i.e., $S2$ for Fig. 9a and $H1$ for Fig. 9b); same arbitrary scale in dB in both figures.

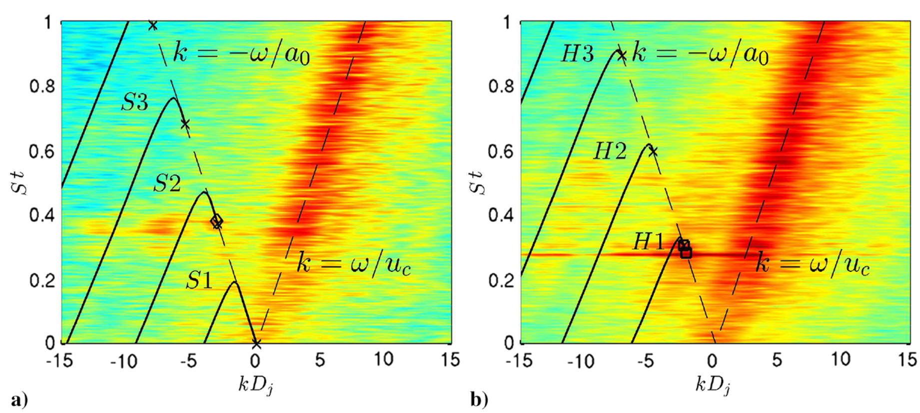

Fig. 10 Frequency-wave-number spectra of density fluctuations at $r = r_0$ for modes of a) $n = 0$ and b) $n = 1$: (solid lines) dispersion relations of a) axisymmetric and b) helical neutral acoustic modes; (×) mode lower limits; (dashed) $k = -\omega/a_0$ and $k = \omega/u_c$; screech tone frequencies for axisymmetric (diamonds) and helical (squares) modes; color-scale levels over 60 dB from blue to red.

the wave number for the main axisymmetric and helical screech mode frequencies for the radial positions of $r = 0.1r_0$, $r = 0.5r_0$, and $r = r_0$. In all cases, the energy peak is found very near the wave number of corresponding upstream-propagating neutral acoustic wave modes $S2$ and $H1$. Finally, at the peak wave numbers, energy is strongest at $r = 0.1r_0$ for the axisymmetric mode in Fig. 9a and at $r = 0.5r_0$ for the helical mode in Fig. 9b. This is consistent with the eigenfunction distributions of modes $S2$ and $H1$ in Fig. 2.

The frequency-wave-number spectra obtained at $r = r_0$ are replotted in Fig. 10 by showing both the negative and the positive wave number parts of the spectra. In this way, both the downstream- and the upstream-traveling waves can be seen. The former waves consist of aerodynamic broadband disturbances convected in the flow direction in the shear layers at an average velocity of $u_c \simeq 0.75u_j$. The latter are acoustic waves propagating at the ambient speed of sound at the screech tone frequencies. They are very likely to close the feedback loop in the jet.

V. Conclusions

In this Note, the origin and the properties of the oscillation modes in screeching, nonideally expanded, round jets are investigated on the basis of the hypothesis of Shen and Tam [8] that the acoustic waves completing the feedback loop in these jets are linked to the upstream-propagating acoustic wave modes of the equivalent ideally expanded jets. Using a jet vortex sheet model to describe the dispersion relations of these modes, it is found that this hypothesis allows us to explain the axisymmetric or helical jet oscillations and the variations with the Mach number of the tone frequencies for screech modes $A1$, $A2$, and u and modes C and c observed in the experiments. For an underexpanded round jet at $\mathcal{M}_j = 1.56$ generating screech tones of modes C and u, which was considered in a previous study [20] using large-eddy simulation, it is also shown that at the screech frequencies, there exist acoustic waves in the jet flow that are propagating in the upstream direction at the ambient speed of sound, which belongs to the neutral acoustic wave modes of the equivalent ideally expanded jet. These results provide strong evidence that a vortex sheet model of the corresponding ideally expanded jet is capable of predicting the wave modes of a nonideally expanded supersonic jet. They also suggest that the feedback path of the mechanism causing screech noise in nonideally expanded jets is achieved, at least for the screech modes mentioned previously, by these waves.

Acknowledgments

The simulation presented in the Note was performed using the High-Performance-Computing resources of the Centre Informatique National de l'Enseignement Supérieur (CINES), under the allocation of 2016-2a0204 made by the Grand Equipement National de Calcul Intensif (GENCI) and of the Swedish National Infrastructure for Computing (SNIC) at the PDC center.

References

[1] Tam, C., "Supersonic Jet Noise," *Annual Review of Fluid Mechanics*, Vol. 27, No. 1, 1995, pp. 17–43.
doi:10.1146/annurev.fl.27.010195.000313

[2] Powell, A., "On the Mechanism of Choked Jet Noise," *Proceedings of the Physical Society. Section B*, Vol. 66, No. 12, 1953, pp. 1039–1056.
doi:10.1088/0370-1301/66/12/306

[3] Raman, G., "Supersonic Jet Screech: Half-Century from Powell to the Present," *Journal of Sound and Vibration*, Vol. 225, No. 3, 1999, pp. 543–571.
doi:10.1006/jsvi.1999.2181

[4] Merle, M., "Sur la Fréquence des Ondes Sonores Émises par un Jet d'air à Grande Vitesse," *Comptes Rendus de l'Académie des Sciences de Paris*, Vol. 243, No. 5, 1956, pp. 490–493.

[5] Davies, M. G., and Oldfield, D. E. S., "Tones from a Choked Axisymmetric Jet. II. The Self Excited Loop and Mode of Oscillation," *Acta Acustica United with Acustica*, Vol. 12, No. 4, 1962, pp. 267–277.

[6] Powell, A., Umeda, Y., and Ishii, R., "Observations of the Oscillation Modes of Choked Circular Jets," *Journal of the Acoustical Society of America*, Vol. 92, No. 5, 1992, pp. 2823–2836. doi:10.1121/1.404398

[7] Tam, C. K. W., Ahuja, K., and Jones, R. R., III, "Screech Tones from Free and Ducted Supersonic Jets," *AIAA Journal*, Vol. 32, No. 5, 1994, pp. 917–922. doi:10.2514/3.12074

[8] Shen, H., and Tam, C., "Three-Dimensional Numerical Simulation of the Jet Screech Phenomenon," *AIAA Journal*, Vol. 40, No. 1, 2002, pp. 33–41. doi:10.2514/2.1638

[9] Tam, C., Seiner, J., and Yu, J., "Proposed Relationship Between Broadband Shock Associated Noise and Screech Tones," *Journal of Sound and Vibration*, Vol. 110, No. 2, 1986, pp. 309–321. doi:10.1016/S0022-460X(86)80212-7

[10] Bogey, C., and Gojon, R., "Feedback Loop and Upwind-Propagating Waves in Ideally-Expanded Supersonic Impinging Round Jets," *Journal of Fluid Mechanics*, Vol. 823, July 2017, pp. 562–591. doi:10.1017/jfm.2017.334

[11] Westley, R., and Woolley, J. H., "The Near Field Sound Pressures of a Choked Jet During a Screech Cycle," *AGARD Conference Proceedings*, Vol. 42, No. 23, 1969, pp. 23.1–23.13.

[12] Panda, J., "An experimental Investigation of Screech Noise Generation," *Journal of Fluid Mechanics*, Vol. 378, Jan. 1999, pp. 71–96. doi:10.1017/S0022112098003383

[13] Lessen, M., Fox, J., and Zien, H., "The Instability of Inviscid Jets and Wakes in Compressible Fluid," *Journal of Fluid Mechanics*, Vol. 21, No. 1, 1965, pp. 129–143. doi:10.1017/S0022112065000095

[14] Tam, C., and Hu, F., "On the Three Families of Instability Waves of High-Speed Jets," *Journal of Fluid Mechanics*, Vol. 201, April 1989, pp. 447–483. doi:10.1017/S002211208900100X

[15] Tam, C. K. W., and Ahuja, K. K., "Theoretical Model of Discrete Tone Generation by Impinging Jets," *Journal of Fluid Mechanics*, Vol. 214, May 1990, pp. 67–87. doi:10.1017/S0022112090000052

[16] Ponton, M., and Seiner, J., "The Effects of Nozzle Exit Lip Thickness on Plume Resonance," *Journal of Sound and Vibration*, Vol. 154, No. 3, 1992, pp. 531–549. doi:10.1016/0022-460X(92)90784-U

[17] André, B., "Etude Expérimentale de L'effet du vol sur le Bruit de Choc de Jets Supersoniques Sous-Détendus," Ph.D. Thesis, École Centrale de Lyon, Ecully Cedex, France, NNT 2012ECDL0042, 2012.

[18] Tam, C. K. W., and Norum, T., "Impingement Tones of Large Aspect Ratio Supersonic Rectangular Jets," *AIAA Journal*, Vol. 30, No. 2, 1992, pp. 304–311. doi:10.2514/3.10919

[19] Gojon, R., Bogey, C., and Marsden, O., "Investigation of Tone Generation in Ideally Expanded Supersonic Planar Impinging Jets Using Large-Eddy Simulation," *Journal of Fluid Mechanics*, Vol. 808, Dec. 2016, pp. 90–115. doi:10.1017/jfm.2016.628

[20] Gojon, R., and Bogey, C., "Numerical Study of the Flow and the Near Acoustic Fields of an Underexpanded Round Free Jet Generating Two Screech Tones," *International Journal of Aeroacoustics*, Vol. 16, Nos. 7–8, 2017, pp. 603–625. doi:10.1177/1475472X17727606

[21] Bogey, C., and Bailly, C., "A Family of Low Dispersive and Low Dissipative Explicit Schemes for Flow and Noise Computations," *Journal of Computational Physics*, Vol. 194, No. 1, 2004, pp. 194–214. doi:10.1016/j.jcp.2003.09.003

[22] Berland, J., Bogey, C., Marsden, O., and Bailly, C., "High-Order, Low Dispersive and Low Dissipative Explicit Schemes for Multiple-Scale and Boundary Problems," *Journal of Computational Physics*, Vol. 224, No. 2, 2007, pp. 637–662. doi:10.1016/j.jcp.2006.10.017

[23] Bogey, C., and Bailly, C., "Large Eddy Simulations of Transitional Round Jets: Influence of the Reynolds Number on Flow Development and Energy Dissipation," *Physics of Fluids*, Vol. 18, No. 6, 2006, Paper 065101. doi:10.1063/1.2204060

[24] Bogey, C., and Bailly, C., "Turbulence and Energy Budget in a Self-Preserving Round Jet: Direct Evaluation Using Large Eddy Simulation," *Journal of Fluid Mechanics*, Vol. 627, May 2009, pp. 129–160. doi:10.1017/S0022112009005801

[25] Fauconnier, D., Bogey, C., and Dick, E., "On the Performance of Relaxation Filtering for Large-Eddy Simulation," *Journal of Turbulence*, Vol. 14, No. 1, 2013, pp. 22–49. doi:10.1080/14685248.2012.740567

[26] Tam, C., and Dong, Z., "Wall Boundary Conditions for High-Order Finite-Difference Schemes in Computational Aeroacoustics," *Theoretical and Computational Fluid Dynamics*, Vol. 6, Nos. 5–6, 1994, pp. 303–322. doi:10.1007/BF00311843

[27] Bogey, C., de Cacqueray, N., and Bailly, C., "A Shock-Capturing Methodology Based on Adaptative Spatial Filtering for High-Order Non-Linear Computations," *Journal of Computational Physics*, Vol. 228, No. 5, 2009, pp. 1447–1465. doi:10.1016/j.jcp.2008.10.042

[28] Bogey, C., Marsden, O., and Bailly, C., "Large-Eddy Simulation of the Flow and Acoustic Fields of a Reynolds Number 10^5 Subsonic Jet with Tripped Exit Boundary Layers," *Physics of Fluids*, Vol. 23, No. 3, 2011, Paper 035104. doi:10.1063/1.3555634

[29] Gojon, R., and Bogey, C., "Flow Structure Oscillations and Tone Production in Underexpanded Impinging Round Jets," *AIAA Journal*, Vol. 55, No. 6, 2017, pp. 1792–1805. doi:10.2514/1.J055618

[30] Panda, J., Raman, G., and Zaman, K. B. M. Q., "Underexpanded Screeching Jets from Circular, Rectangular and Elliptic Nozzles," AIAA Paper 1997-1623, 1997. doi:10.2514/6.1997-1623

[31] Towne, A., Cavalieri, A. V. G., Jordan, P., Colonius, T., Schmidt, O., Jaunet, V., and Brès, G., "Acoustic Resonance in the Potential Core of Subsonic Jets," *Journal of Fluid Mechanics*, Vol. 825, Aug. 2017, pp. 1113–1152. doi:10.1017/jfm.2017.346

D. Gaitonde
Associate Editor